Control, Propulsion and Energy Assessment of a Spherical UAS for Low Speed Operations

BANDYCKI, Sebastian, TRANCOSSI, Michele and PASCOA, Jose

SAE INTERNATIONAL®

Control, Propulsion and Energy Assessment of a Spherical UAS for Low Speed Operations

2017-01-2065

Published 09/19/2017

Sebastian Bandycki
Independent researcher

Michele Trancossi
Sheffield Hallam Univ.

Jose Pascoa
Universidade Da Beira Interior

CITATION: Bandycki, S., Trancossi, M., and Pascoa, J., "Control, Propulsion and Energy Assessment of a Spherical UAS for Low Speed Operations," SAE Technical Paper 2017-01-2065, 2017, doi:10.4271/2017-01-2065.

Abstract

This paper presents a comparison between different hypotheses of propulsion of a spherical UAS. Different architectures have been analyzed assessing their specific aerodynamic, energetic, and flight mechanics features. The comparison has been performed assuming the robustness of flight control in different wind conditions, defining for each the specific operative ranges, mission profiles, and energy assessment. An effective energy assessment and comparison against a commercial UAS has been produced. Even if the paper considers a preliminary simplified configuration, it demonstrates clearly to be competitive against traditional quadcopters in a predefined reference mission.

Introduction

This paper presents a new UAS concept. It is new design spherical drone taking advantage of a series of innovation with respect to any possible competitor. The specific aircraft has a new propulsion system that s based on Coanda effect and take advantage of the induced supercirculation. The propulsion is ensured my mean of a series of air jets on the surface explicating a former concept that was defined by Coanda in one of his patents.

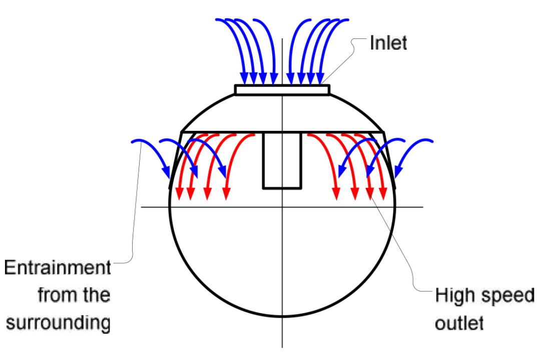

Figure 1. Preliminary concept drawing

The above preliminary concept has been directly exploited from a former patent by Henri Coanda [1].

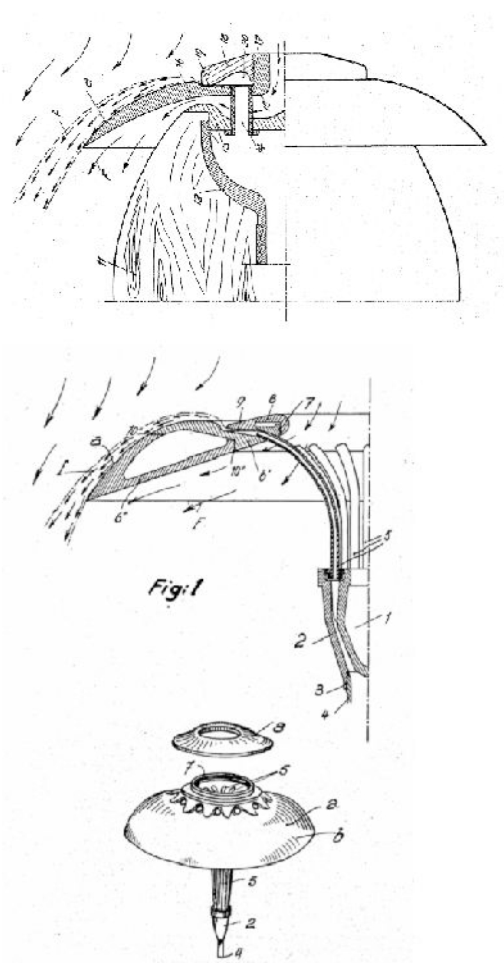

Figure 2. Henry Coanda lifting device patent [1]

The idea is to produce a spherical drone that can safely flight safely over people and in aggressive environment, such as the presence of high temperatures, pollutants, electromagnetic radiation, minimizing the risk for men in environments, which cannot be explored by ground based robots because of their nature, and present problems for the activities of traditional drones.

It is well known that a sphere is not optimized for flight, but, as research on flying saucers unconventional air vehicles demonstrates, can produce generate interesting vehicle concepts.

A later patent by Coanda [2] presents a control system and method for unconventional flying saucers that is based on the compositions of the thrust produced by means of a number of jet propellers placed on the external section of the flying saucer.

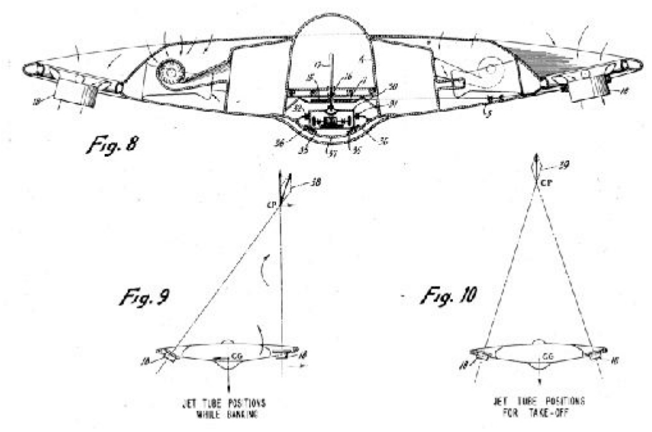

Figure 3. Coanda device for the simultaneous control of lifting and directional elements [2].

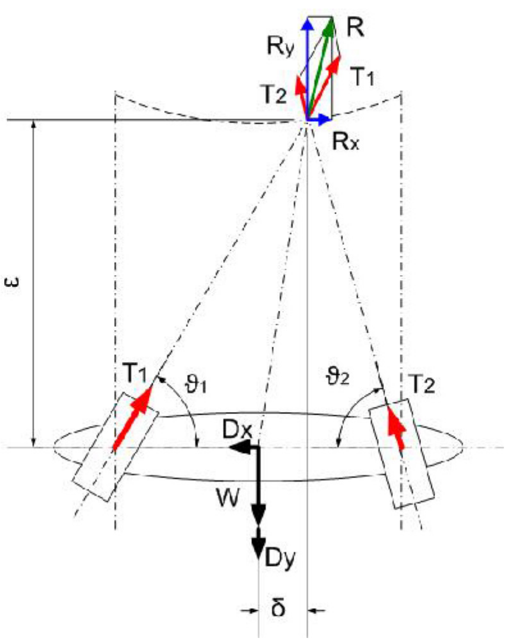

Figure 4. A preliminary model derived from Coanda patent [2]

This patent allows assimilating the flight motion rules for a flying saucer to the ones that applies to a helicopter (Figure 3 images Fig. 9 and Fig. 10). A sketch that explains the hypothesis by Coanda by evidencing the different forces is provided in figure 4.

The equation of flight on a vertical plane of the object can be derived by the ones of a helicopter by considering the schema in figure 4. Assuming a symmetric shape aerodynamic lift is neglected.

$$\begin{cases} Ma_x = \Sigma_i Fx \\ Ma_y = \Sigma_i F_y \\ I\dot{\omega}_z = \Sigma_i M_z \\ 0 = \Sigma_i M_y \end{cases} \Rightarrow \begin{cases} m\ddot{x} = T_1 \cos\vartheta_1 - T_2 \cos\vartheta_2 - D_x \\ m\ddot{y} = T_1 \sin\vartheta_1 + T_2 \sin\vartheta_2 - W - D_y \\ I\dot{\omega}_z = -\delta \cdot \left(T_1 \sin\vartheta_1 + T_2 \sin\vartheta_2\right) \\ \qquad + \varepsilon \cdot \left(T_1 \cos\vartheta_1 - T_2 \cos\vartheta_2\right) \\ M_p + M_r = 0 \end{cases} \tag{1}$$

If we consider the helicopter energy model defined by Wood [3] and Zuang [4], the energy state of a helicopter during flight is given by equation (1):

$$E = \frac{1}{2} m\dot{x}^2 + mgh + \frac{1}{2} I\Omega^2 . \tag{2}$$

By taking the partial derivative with respect to time of equation 1, the energy rate is expressed as:

$$\dot{E} = m \cdot \dot{x} \cdot \ddot{x} + m \cdot g \cdot \dot{y} + I \cdot \Omega \cdot \dot{\Omega} \tag{3}$$

In which it can be assumed that the angular acceleration is negligible against other terms. Equation (3) reduces to the following:

$$\dot{E} = m \cdot \dot{x} \cdot \ddot{x} + m \cdot g \cdot \dot{y} \tag{3'}$$

Other Flying Saucer Concepts

Probably the first related concept has been the aeronautical machine by Robinson [5].

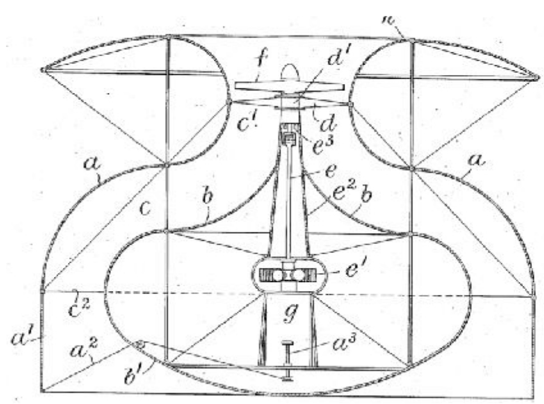

Figure 5. Aeronautical Machine by Robinson [5]

Sharpe [6] proposes and evolution of the Coanda's lifting device [1] concept.

Crabtree [7] has developed a wingless heavier than air aircraft, in which the fuselage is generally flat, and is annular in configuration. This aircraft could travel vertically as well as laterally, and which is provided with means for controlling the tilt thereof.

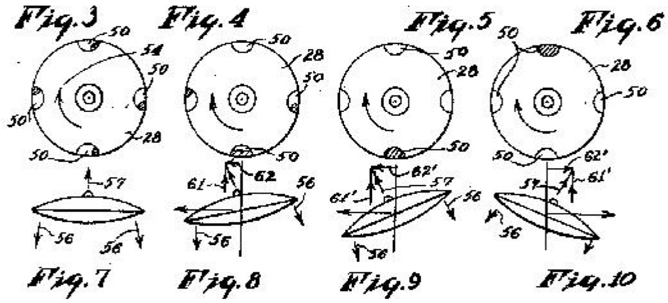

Figure 6. Fluid sustained and pan annular shaped bodyaving annular shaped body [6]

One interesting flying saucer concept has been patented by Mulgrave and Ringlieb [8]. This invention relates to a flying sauced shaped compact integral structure with an interior fluid impelling apparatus that derives sufficient lift to provide vertical takeoff and landing.

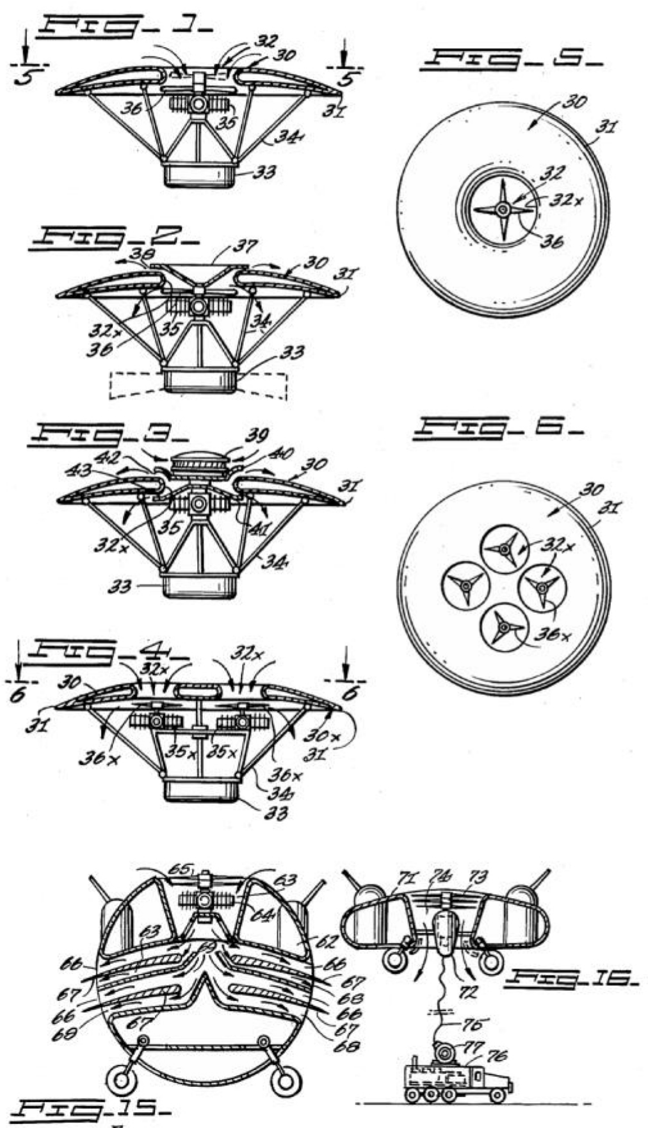

Figure 7. The discord airfield vehicle concept [8]

Lent [8] has elaborated a circular wing aircraft elaborating the originals Coanda [1] and Robinson's [5] concepts. In particular, it presents an interesting nearly spherical architecture (Fig. 15) the reference directly the actual vehicle concept that is the argument of this aircraft.

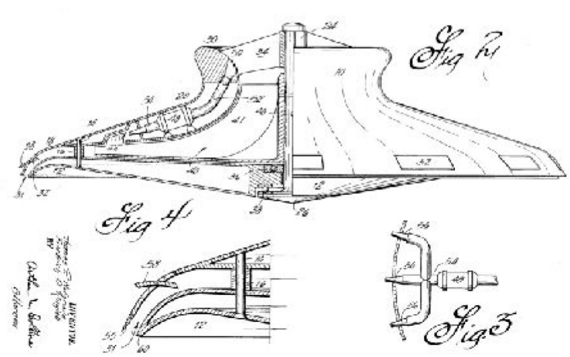

Figure 8. Mulgrave and Ringlieb flying saucer

Mulgrave and Ringlieb [9] present a concept based on a vertical axis rotor and embedded jets to allow the flight of a new concept of flying saucers.

Louvel [10] has designed an electrical remote-control and remote-power flying saucer (figure 8).

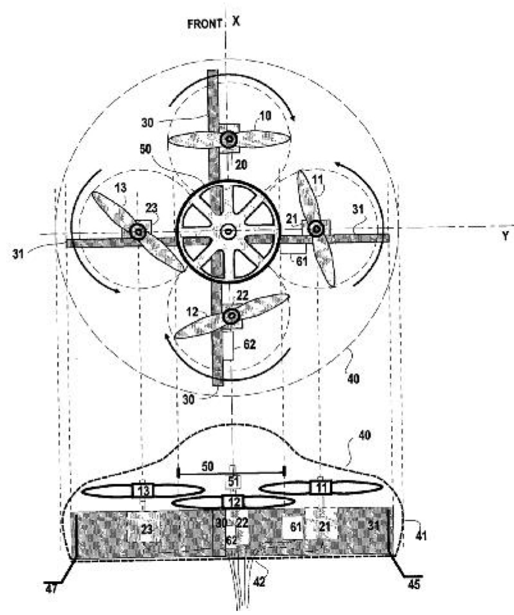

Figure 9. Multicopter based flying electrical flying saucer. [10]

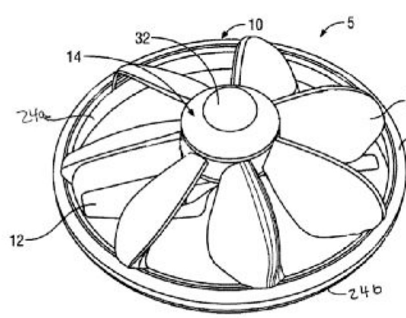

Figure 10. Davis directionally controllable propelled circular vehicle.

Davis [11] has developed the concept of a directionally controllable flying vehicle and a propeller mechanism for accomplishing the same." U.S. Patent 8,272,917, issued September 25, 2012.

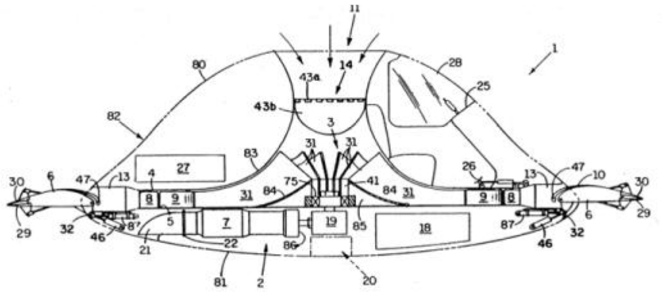

Figure 11. VTOL aircraft by Beck

Beck has patented a VTOL aircraft concept that improves the idea of Mulgrave and Ringlieb by introducing lateral flapping winglets.

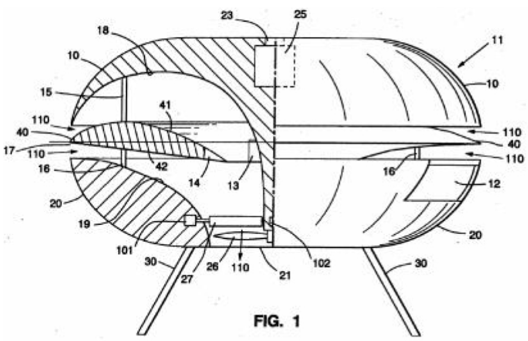

Figure 12. Fixed circular wing aircraft [13]

Bose [13] has patented an interesting fixed wing aircraft, but still with some limits in manoeuvrability.

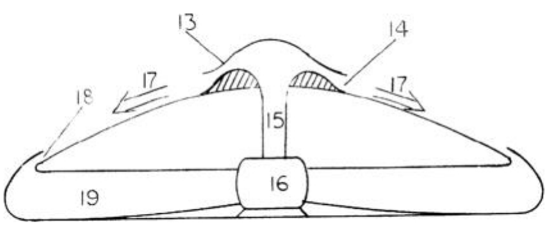

Figure 13. Aerodynamic lift apparatus [14].

Chen [14] has patented a very interesting lifting concept based on Coanda effect fluid stream over the top surfaces of the vehicle. It produces the lift by mean of using the method of blowing air over the upper surface of the vehicle to generate lift by virtue of the balance of outside pressures against the body of the vehicle.

Even if not directly related to the aeronautic sector, the Dyson bladeless ventilator regards the arguments of the present study. It presents a fan assembly for creating an air current by a bladeless fan assembly, including a nozzle and a device for creating an air flow through the nozzle. The nozzle includes an interior passage and a mouth receiving the air flow from the interior passage. A Coanda surface located adjacent the mouth and over which the mouth is arranged to direct the air flow. The fan provides an arrangement producing an air current and a flow of cooling air created without requiring a bladed fan, that is, the air flow is created by a bladeless fan.

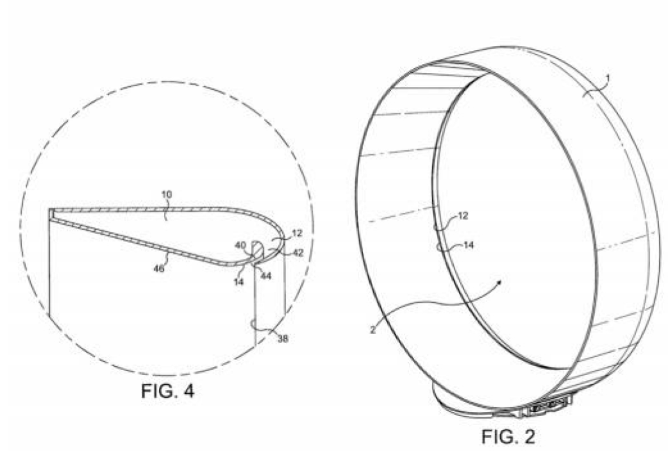

Figure 14. Dyson Bladeless fan [15]

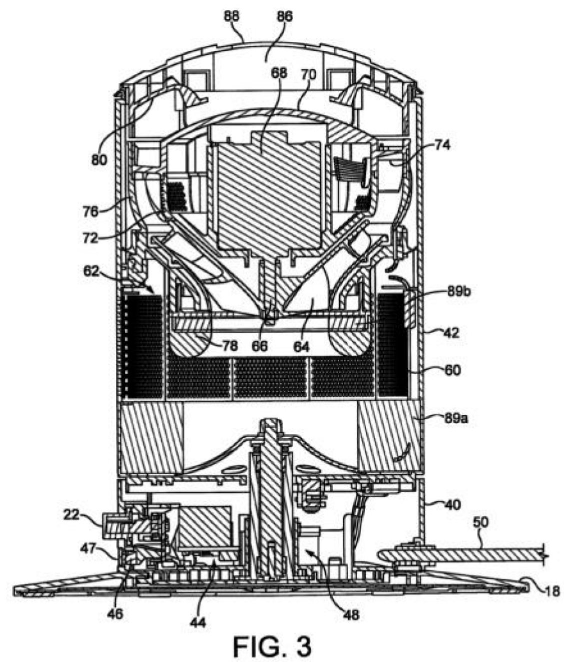

Figure 15. Compressor of the Dyson bladeless ventilator [15]

An interesting attempt of assessing the propulsion for an almost spherical vehicle has been defined by Hatton [16].

There have been past proposals for air vehicles employing the Coanda effect. A jet of fluid, usually air, has blown in radial direction outwardly over a dome-shaped canopy to create lift. A cross-section through the canopy is curved to follow a segment of a circle or it may have a radius of curvature that increases in the direction of flow. The radius (r) of the canopy curve decreases towards the downstream direction (x) in a way that is related to the decrease in the width of the jet as it flows over the surface. This means that the radius of curvature decreases (instead of increasing) towards the downstream direction with the rate of decrease being progressively less rapid towards the downstream direction. This kind of shape allows a better aerodynamic adherence of the fluid to the canopy and increases consequently Coanda effect.

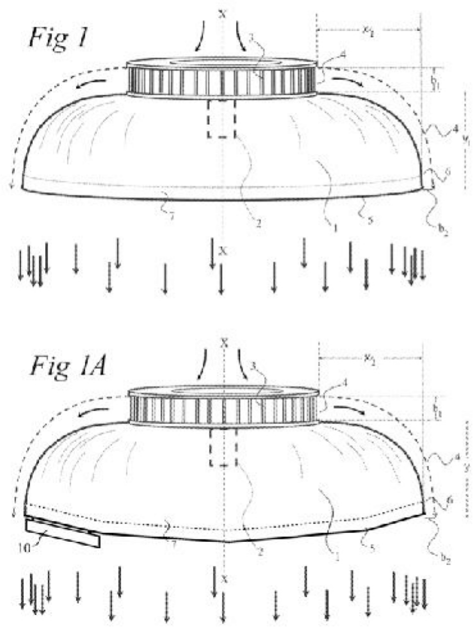

Figure 16. The two configurations of Hatton Patent. [15]

Definition of the Propulsion System for a Spherical Object

The above analysis of some of the most relevant configurations, which have been defined, constitutes a good basis for the study of the specific problem of the propulsion of a spherical air vehicle.

The design method is derived from the optimization of the equations of motions such as in Trancossi et al. [18]. This method is an improvement of second principle analysis [19] according to the EMIPS method [20] as adapted by Trancossi [21, 22]. It is then a method defined on the flight mechanics equations and energy equations of the system, to define a preliminary optimal configuration that can be then designed and tested.

Considering the equation of motion it is evident that a vehicle with almost zero aerodynamic speeds, such as a flying sphere is, a certain amount of power must be used for keeping the aircraft in flight conditions.

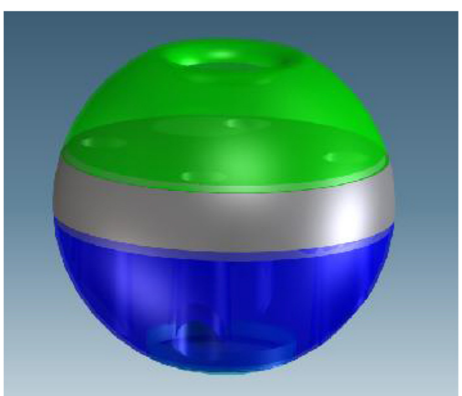

Figure 17. Preliminary 3D rendering of the spherical drone.

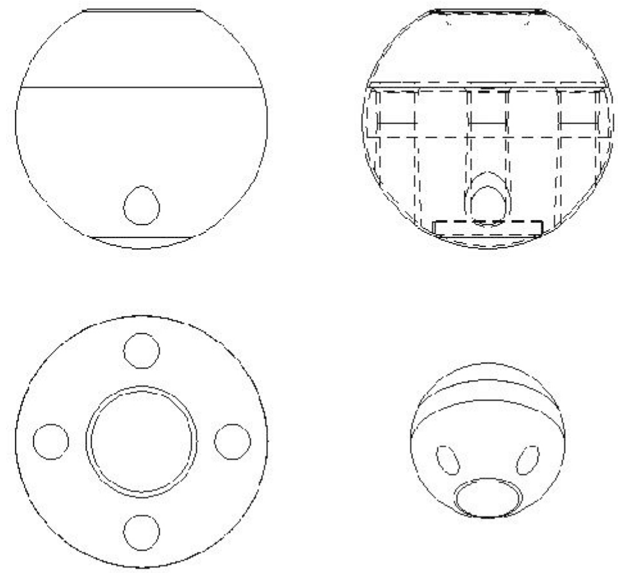

Figure 18. Preliminary system cad drawing.

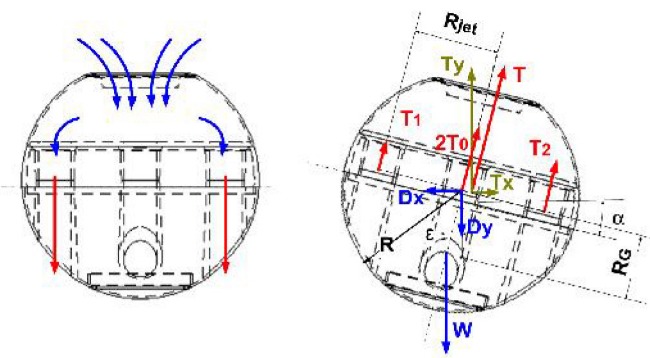

Figure 19. Principle of operations: schema of fluid flows; schema of applied forces.

The choice of a ducted fan system has been originated by two different reasons:

1. The duct provides vectored thrust, which increases propulsive efficiencies while adding to lateral and longitudinal stability [32].
2. The duct surrounds the prop, which reduces the noise caused by tip effects.

The system is subject to a 3D system of parallel forces. In the case of motion on a flat plane, and assuming that T_0 has a null moment with respect to the centre of gravity G, the resultant force is the sum of the forces T_1, T_2, and $2T_0$. Its line of action can be determined by the equilibrium of momentums or by the graphical equilibrium of T_1 and T_2. The resultant will lie at a distance δ from the centre of the sphere on the side of the largest force.

Flight Model

Such as a helicopter the system will be obliged to assume a negative angle of attack α, such as in a helicopter that allows having a resultant force, which equals the drag and the weight components. It must ensure the equilibrium of the forces against rotation that depends on the intensity of T_1 and T_2. In particular, the weight force will be moved against the vertical of a distance ε, which is a function of both R_G and α. Assuming

1. $T_1 + T_2 = 2T_0$
2. $T_1 - T_2 = 2\Delta T \rightarrow \begin{cases} T_1 = T_0 + \Delta T \\ T_2 = T_0 - \Delta T \end{cases}$
3. $T = T_1 + T_2 + 2T_0 = 4T_0$
4. $\varepsilon = R_G \cdot \sin \alpha$
5. $\delta = R \cdot \dfrac{T_2 - T_1}{T_2 + T_1} = R \cdot \dfrac{\Delta T}{T_0}$

A specific flight model can be possible assessed by adopting the equations of the dynamic of the system according to Newton's second law on a 2D plane that reduces to:

$$\begin{cases} m\ddot{x} = T\sin\alpha - D_x \\ m\ddot{y} = T\cos\alpha - W - D_y \\ I\ddot{\alpha} = \delta \cdot T - R_G \sin\alpha \cdot D_y + R_G \cos\alpha \cdot D_x \end{cases} \tag{1}$$

The net thrust of a ducted fan unit can then be expressed as:

$$T = \dot{m}_{air}(u_e - u_0) \tag{2}$$

Consequently, the power imparted to the fluid is:

$$P = \dot{m}_{air}\left(\frac{u_e^2}{2} - \frac{u_0^2}{2}\right) \tag{3}$$

Considering the propeller it can be possible to write the thrust as:

$$T = k_T \cdot \rho \cdot n^2 \cdot D^4 \tag{4}$$

and the torque applied to the propeller as

$$Q = k_Q \cdot \rho \cdot n^2 \cdot D^5 \tag{5}$$

It can be then possible to express the power input as

$$P_{in} = 2\pi \cdot n \cdot Q = k_P \cdot \rho \cdot n^2 \cdot D^5 \tag{6}$$

in which

$$k_P = 2\pi \cdot k_Q$$

Consequently, it can be possible to consider the total propulsive efficiency as:

$$\eta_{prop} = \frac{u_e}{2\pi \cdot n} \cdot \frac{k_T}{k_P} = J \cdot \frac{k_T}{k_P}$$

Equation of motion in horizontal motion reduces to:

$$\begin{cases} m\ddot{x} = T\sin\alpha - D_x \\ T\cos\alpha - W - D_y = 0 \\ \delta \cdot T - R_G \sin\alpha \cdot D_y + R_G \cos\alpha \cdot D_x = 0 \end{cases}$$

in vertical motion to

$$\begin{cases} T\sin\alpha - D_x = 0 \\ m\ddot{y} = T\cos\alpha - W - D_y \\ \delta \cdot T - R_G \sin\alpha \cdot D_y + R_G \cos\alpha \cdot D_x = 0 \end{cases}$$

And in case of stabilization

$$\begin{cases} T\sin\alpha - D_x = 0 \\ T\cos\alpha - W - D_y = 0 \\ I\dot{\omega}_z = \delta \cdot T - R_G \sin\alpha \cdot D_y + R_G \cos\alpha \cdot D_x \end{cases}$$

In addition, an accurate 3D model can be produced, but those equations are sufficient to produce an energy flight model for the specified system.

Energy Model

A measure of the energy state of a helicopter [9] is given by equation (2) at any altitude and airspeed-RPM combination, and by (3) and (3') in term of power.

Power can be expressed by the simplified equations by McCormick [8] for horizontal flight.

$$\dot{E}_x = P_x = P_{x,o} + \frac{1}{2} \cdot \frac{(m \cdot g)^2}{\rho \cdot A_f \cdot V_x} + \frac{1}{2} \cdot \rho \cdot C_{D,x} \cdot A_f \cdot V_x^3 \tag{8}$$

and for vertical flight

$$\dot{E}_y = P_y = V_y \cdot \left(mg + \frac{1}{2} C_{D,y} A_t \rho V_y\right). \tag{9}$$

Total power is consequently

$$P_{tot} = P_x + P_y \tag{10}$$

The total power required is obtained by rotor power and overall efficiency factor η is

$$P_{req,tot} = \eta \cdot P_{req,rot}\,. \tag{11}$$

Optimization of Helicopter Equations

By equations (4) and equations (8) and (9), it is possible to produce a preliminary abstract optimization of a theoretical system that can act as according to those equations and then performing the same operations that a helicopter does. Starting from the optimization of the system of forces that may be produced by a hypothetical flying vehicle that can act as a helicopter it is immediate to observe that the best conditions are the ones that allow minimizing thrust or moment in any direction.

Analysis of Forces and Moments

Equation of rotation around a vertical axis shows clearly that avoidance of the propulsion system with a vertical axis of rotation allows making null the rear rotor moment. Equation of rotation around z-axis shows that it can minimize thrust by an aerodynamic system that can grant an adequate momentum by mean of aerodynamic lift by wings or ailerons. A similar conclusion is obtained by the equation of vertical motion. The vertical thrust $T_y = T\cos\phi$ lowers by both increasing the vertical lift by aerodynamic surfaces and lowering the vertical drag. The equation of horizontal motion shows that the minimization of horizontal thrust requires the minimization of horizontal drag.

Energetic Model

Further analysis will relate to the energy analysis of the system. The power equation found in traditional bibliography, which have been cited in the preceding paragraph, can be improved by a more accurate analysis according to Trancossi [4, 9, and 10].

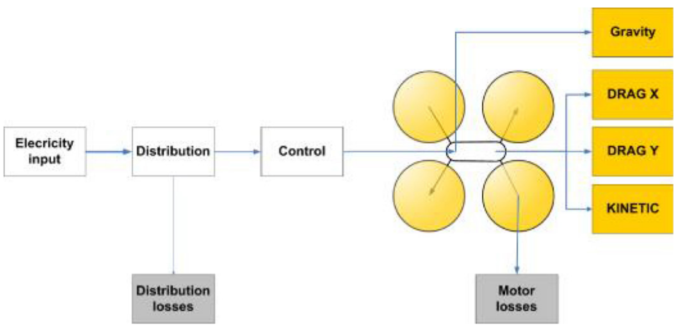

Figure 20. Energy dissipations in a multicopter

Figure 20 shows energy losses for the moving vehicle. A schema of the powertrain indicating the different losses is provided in Figure 2. Losses depend on the flight condition in which the helicopter operates.

For simplicity, the model will be developed neglecting minor energy components and assuming that vertical lift force is mostly produced by propulsion and not by aerodynamic appendices. Applying this model, it is evident that the energy components that have to be considered are more complex with respect to other transport modes. They are:

$$E_{K,x} = \frac{1}{2} m v_x^2; E_{K,y} = \frac{1}{2} m v_y^2$$

$$L_{T,x} = \int_0^{t_{tot}} T_x v_x dt; L_{T,y} = \int_0^{t_{tot}} T_y v_y dt$$

$$L_{D,x} = \int_0^{t_{tot}} \left(\frac{1}{2} C_{D,x} \rho A v_x^2 \right) v_x dt; E_{D,y} = \int_0^{t_{tot}} \left(\frac{1}{2} C_{D,y} \rho A v_y^2 \right) v_y dt$$

$$E_{P,y} = mgh$$

$$E_{R,p} = \frac{1}{2} I_p \Omega_p^2; E_{R,r} = \frac{1}{2} I_r \Omega_r^2$$

The evaluation of exergy needs for moving can be performed by equation (12)

$$Ex_{service} = m_{tot}\left(gh + \frac{1}{2} v_{\max,x}^2 + \frac{1}{2} v_{\max,y}^2 \right) + \frac{1}{2} C_{D,x} A_x \rho_{air} v_{av,x}^3 t_x + \frac{1}{2} C_{D,y} A_y \rho_{air} v_{av,y}^3 t_y + \frac{1}{2} I_p \Omega_p^2 + \frac{1}{2} I_r \Omega_r^2 \tag{12}$$

Equation (12) can be divided into two equations, one related to the vehicle and one to the payload:

$$Ex_{veh} = m_{veh}\left(gh + \frac{1}{2} v_{\max,x}^2 + \frac{1}{2} v_{\max,y}^2 \right) + \frac{1}{2} C_{D,x} A_x \rho_{air} v_{av,x}^3 t_x + \frac{1}{2} C_{D,y} A_y \rho_{air} v_{av,y}^3 t_y + \frac{1}{2} I_p \Omega_p^2 + \frac{1}{2} I_r \Omega_r^2 \tag{13}$$

$$Ex_{pay} = m_{pay}\left(gh + \frac{1}{2} v_{\max,x}^2 + \frac{1}{2} v_{\max,y}^2 \right) \tag{14}$$

It can be also possible to write express energy losses of the engine and power train:

$$Ex_{vehicle} = Ex_{fuel} - L_{engine} - L_{standby} - L_{Powertrain} \tag{15}$$

Equations (12), (13) and (14) allow analysing the performances in service conditions during operations of the vehicle. In particular, the equations (13) and (14) allow expressing the energy consumption required for moving the vehicle and the payload.

Energy Optimization

The above model allows an effective energy optimization of a vehicle that virtually can operate according to the same physical laws that applies to a helicopter. By the preliminary evaluations made on forces and moments it can be possible to perform a preliminary minimization of the terms that appear in the energy balance:

$$Ex_{service} = m_{tot}\left(\frac{1}{2} v_{\max,x}^2 + \frac{1}{2} v_{\max,y}^2 \right) + \frac{1}{2} C_{D,x} A_x \rho_{air} v_{av,x}^3 t_x + \frac{1}{2} C_{D,y} A_y \rho_{air} v_{av,y}^3 t_y \tag{16}$$

It simplifies during horizontal flight:

$$Ex_{service} = m_{tot}\left(\frac{1}{2} v_{\max,x}^2 \right) + \frac{1}{2} C_{D,x} A_x \rho_{air} v_{av,x}^3 t_x$$

Equation (16) can describe the system behaviour of a vehicle during horizontal flight and lift operations. It could not describe the energy equilibrium during vertical lift and during hovering. Those operations can be described by the equation (17)

$$Ex_{service} = m_{tot}\left(gh + \frac{1}{2} v_{\max,y}^2 \right) + \frac{1}{2} C_{D,x} A_x \rho_{air} v_{av,x}^3 t_x + \frac{1}{2} C_{D,y} A_y \rho_{air} v_{av,y}^3 t_y \tag{17}$$

It is necessary to consider the component that relates to horizontal drag, because it is not frequent to be in the condition of ideal calm air. However, this component can be neglected with very low airspeeds around the vehicle

Preliminary Benchmark Case

A sphere with a diameter of 500 mm made by a 1 mm rotation moulding PET bodies has been assumed. Installed fans are RC Lander 70mm 3200kv 4S Lipo EDF with a 2839L 3200KV Brushless Outrunner motor.

The comparison will be conducted against one of the more successful drones ever built for professional use with interesting results.

The comparison has been produced according to equation (10) that present the formulation of exergy dissipations according EMIPS model [19] and revised by Trancossi [20, 21].

This comparison has just the meaning of a comparison in terms of performances, but do not consider the fact that the two vehicles have very different missions and objectives.

Table 1. Sphere vs. DIJ inspire quadcopter technical data

		DJI Inspire pro	Sphere UAS
	units		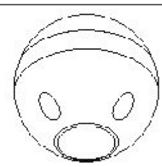
Length	*mm*	750	500
Width	*mm*	430	500
Height	*mm*	246	475
Propulsions			
Motor	-	4x DJI 3510H 6s 420 kV	2839L 3200KV Brushless Outrunner
Propeller	-	4 x DJI 1345T	4 x RC Lander 70mm 3200 kV
Batteries			
		DJI Intelligent Flight Battery TB47	Multistar HC 5200mAh 4S 10C Multi-Rotor Lipo
Voltage	*V*	22.2	14.8
Capacity	*mAh*	4500	5200
Net Weight	*kg*	0.57	0.45
Energy	*Wh*	99.9	76
Residual capacity	*%*	85	85
Weights			
Empty weight	*kg*	2.87	2.80
Payload	*kg*	0.63	0.70
MTOW	*kg*	3.5	3.5
Performances			
Max speed	*m/s*	22	15
Max wind res.	*m/s*	10	10
Max vert. speed	*m/s*	2	2
Max ang. Vel.			
Pitch	*°/s*	300	150
Yaw	*°/s*	150	150

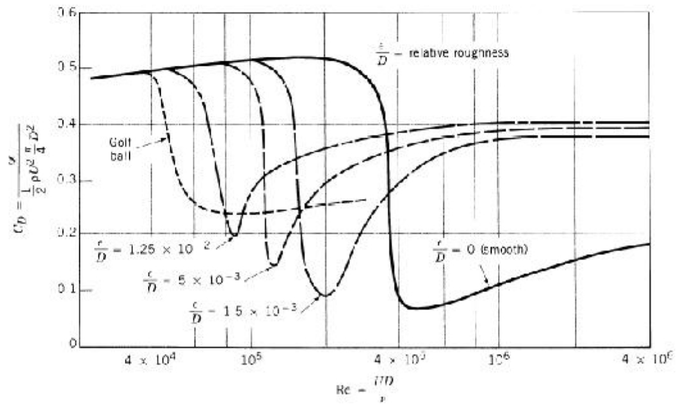

Figure 21. The C_D coefficient as a function of roughness for different spherical objects [25].

For the needs of this preliminary analysis, it has been assumed a CD of the Spherical object as obtained by preliminary CFD analysis equal to 0.36 which is in line with the actual CD of a sphere [24] (about 0.5 for Re > 5 10^3). By considering Monson [25] it can decrease with the surface roughness (Figure 21). The claimed value in then in line with the values of roughness for a superficial roughness ε/D = 1.25 x 10^{-2}.

Results

According to Johnson and Turbe [23], it is possible to assess the power need of the vehicle by modelling the electric ducted fan units.

By the preliminary defined method, it is possible to assess an effective comparison on a defined mission for both vehicles they have been assessed according to the cited method and compared against Dietrich [26] and Shi [27]. The mission has been defined in indoor conditions. Vertical speed has been defined in 1 m/s. Average flight speed has been assumed equal to 5 m/s. Values for the Results have been evaluated conservatively and have been reassumed in Table 2. They clearly show that the system can be competitive against traditional drones in terms of energy consumption, notwithstanding the configuration is still far from an optimal one.

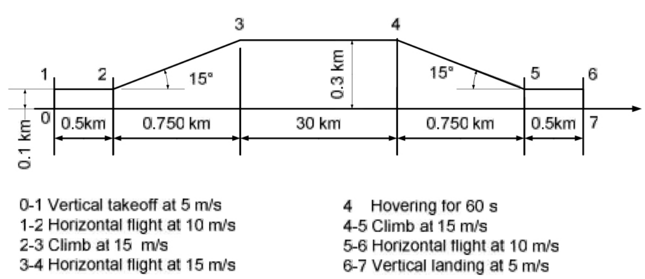

Figure 22. Mission Profile

They clearly demonstrate that a spherical drone, even in a not optimized architecture can ensure energetic performances, which are inline with a traditional multicopter.

If the results are compared with the battery capacity it can be clearly demonstrated that the actual spherical drone configuration have a potential time of flight in the range of 15/20 min, which is analogous to the one of the reference multicopter.

Table 2. Comparison of ideal calculated performances of multicopter against spherical drone.

		Air speed	Length	Height change	Time	Multicopter		Sphere	
						Power	Energy	Power	Energy
		(m/s)	(m)	(m)	(s)	(W)	(kJ)	(W)	(kJ)
Vertical take off	P0-1	2	100	100	50	82	4.1	74	3.7
Horizontal flight	P1-2	5	500	0	100	206	20.6	218	21.8
Climb	P2-3	5	772.5	200	154.5	206	31.8	206	31.8
Horizontal Flight	P3-4	10	1000	0	100	412	41.2	453	45.3
Hovering	P4	0	0	0	30	72	2.2	72	2.2
Descent	P4-5	5	772.5	-200	154.5	206	31.8	206	31.8
Horizontal flight	P2-4	5	500	0	100	206	20.6	218	21.8
Vertical landing	P0-3	2	100	-100	50	70	3.5	65	3.3
Average values		**6.17**				**183**		**189**	
Total significant values			**3745**	**0**	**739**		**155.8**		**161.8**

This paper has considered a very basic preliminary version of the required drone. A more accurate aerodynamic definition both in terms of propulsion (improving it by mean of Coanda effect) or in terms of a better definition of the surfaces could generate future significant improvements, which are expected to be in line or improve the theoretical model of the multicopter.

Conclusions

This paper, after a large bibliography and patenting reference analysis, produces a preliminary energy assessment of an initial even if not optimized architecture of a possible spherical UAS that can be used for different possible future uses in the area of safety, security, vigilance and monitoring.

This vehicle concept presents a major benefit with respect to any traditional multicopter because of an effective inoffensive design that can allow operating also over the people. Further uses can deal with an effective use in hostile environments such as in the presence of atmospheric chemical pollution.

The energy assessment made against a market leader commercial UAS with the same expected weight demonstrates the system feasibility of the proposed drone demonstrating that their energy consumptions are fundamentally similar on the same reference mission.

These preliminary results can be easily extended also to future more evolved vehicle concepts, which can be derived from further improvements of the performances. Future and more evolved versions are expected to improve their performances by a better positioning of the propeller and a better shaping of the vehicle.

References

1. Coanda, H., "Propelling device." U.S. Patent 2,108,652, issued February 15, 1938.
2. Coanda, H. "Device for the simultaneous control of lifting and directional elements." U.S. Patent 2,939,654, issued June 7, 1960.
3. Wood T L, Livingston C L, An energy method for prediction of helicopter maneuverability AD Report, ADA021266, 1971.
4. Zhuang N, Xiang, J. et al., "Calculation of helicopter maneuverability in forward flight based on energy method", Computer Modelling & New Technologies, 18(5) 50-54, 2014.
5. Robertson, P.J., "Construction of aeronautical machines." U.S. Patent 1,123,589, 1915.
6. Sharpe, C. D., "Aerodynamic impelling device." U.S. Patent 2,468,787, 1949.
7. Crabtree, E.L., "Fluid sustained and propelled aircraft having annular shaped body." U.S. Patent 2,718,364, 1955.
8. Lent, C. P., "Aircraft with discoid sustaining airfoil." U.S. Patent 3,034,747, 1962.
9. Mulgrave, T. P., and Ringleb, F.O., "Gyro stabilized vertical rising vehicle." U.S. Patent 2,997,254, 1961.
10. Louvel, P., "Electrical remote-control and remote-power flying saucer." U.S. Patent Application 10/048,091, filed April 5, 2001.
11. Davis, S., "Directionally controllable flying vehicle and a propeller mechanism for accomplishing the same." U.S. Patent 8,272,917, 2012.
12. Beck, A.H. Jr, "VTOL aircraft." U.S. Patent 5,170,963, 1992.
13. Bose, P. R., "Fixed circular wing aircraft." U.S. Patent 5,046,685, 1991.
14. Chen, C., "Aerodynamic lift apparatus." U.S. Patent 6,073,881, 2000.
15. Dyson, J., et al. "Fan." U.S. Patent D602,144, 2009.
16. Dyson, J., et al. "A Fan." U.S. Patent D602,144, 2010.
17. Hatton, G., "Thrust generating apparatus." U.S. Patent 7,857,256, issued December 28, 2010.
18. Trancossi, M., Stewart, J. and Pascoa, J.C., 2016, November. A New Propelled Wing Aircraft Configuration. In ASME 2016 International Mechanical Engineering Congress and Exposition. American Society of Mechanical Engineers 2016, p. V001T03A048. doi:10.1115/IMECE2016-65373
19. Gong M., Wall G., “On exergy and sustainable development-Part 2: Indicators and methods”, Exergy, An International Journal, Volume 1, Issue 4, 2001, P. 217-233.
20. Dewulf J, and Van Langenhove H., “Exergetic material input per unit of service (EMIPS) for the assessment of resource productivity of transport commodities”. Resources Conservation and Recycling. 38(2), Pages: 161-174 (2003).
21. Trancossi, M., "A response to industrial maturity and energetic issues: a possible solution based on constructal law." European Transport Research Review 7, no. 1 (2015): 1-14. doi:10.1007/s12544-014-0150-4.
22. Trancossi, M., "What price of speed? A critical revision through constructal optimization of transport modes." International Journal of Energy and Environmental Engineering 7.4, 2016, pp.425-448. doi:10.1007/s40095-015-0160-6

23. Johnson, E.N. and Turbe, M.A., "Modeling, control, and flight testing of a small-ducted fan aircraft." Journal of guidance, control, and dynamics, 29(4), 2006. pp.769-779.
24. Çengel, Y. A. and Cimbala, J. M., "Fluid Mechanics - Fundamentals and Applications," McGraw-Hill, NY, 2006.
25. Munson, B. R., Young, D. F., and Okiishi, T. H., "Fundamentals of Fluid Mechanics," Wiley, NY, 1990.
26. Dietrich, T., Krug, S. and Zimmermann, A., An Empirical Study on Generic Multicopter Energy Consumption Profiles.

Contact Information

Sebastian Bandycki
HAXTRON
http://haxtron.com/
seb@haxtron.com
phone: (+353) 866019005

Michele Trancossi
Sheffield Hallam University
m.trancossi@shu.ac.uk
mtrancossi@gmail.com

Definitions/Abbreviati1ons

CD - Drag Coefficient (-)

CL - Lift Coefficient (-)

$\mathbf{k_t}$ - Thrust coefficient

$\mathbf{k_p}$ - Power coefficient,

$\mathbf{k_Q}$ - Torque coefficient

δ - Distance between vertical thrust and centre of gravity (m)

ε - distance between the point of application

α - Pitch angle (rad)

Ω - Angular velocity of helicopter propeller (rad/s)

ρ - Density (kg/m3)

A - Area (m2)

D - Drag force (N)

E - Energy (J)

Ex - Exergy (J)

I - Moment of Inertia (kg m2)

Ip - moment of inertia of main propeller (kg m2)

L - Lift Force (N)

P - Power (W)

R - Rotor Radius (m)

T - Thrust (N)

V - Air speed (m/s)

a - Acceleration (m/s2)

g - Gravity (9.81 m/s)

h - Height (m)

m - mass (kg).

t - Time (s)

v - Velocity (m/s)

EMIPS - Exergetic Material Input per Unit of Service (J)

D - drag (related to energy and power)

K - kinetic (related to energy and power)

R - rotor (related to energy and power)

T - Thrust (related to energy and power)

req - required

rot - rotor

x - horizontal

y - vertical

The Engineering Meetings Board has approved this paper for publication. It has successfully completed SAE's peer review process under the supervision of the session organizer. The process requires a minimum of three (3) reviews by industry experts.

ISSN 0148-7191

http://papers.sae.org/2017-01-2065